Magnetowave Induced Plasma Wakefield Acceleration for Ultrahigh Energy Cosmic Rays

Feng-Yin Chang,[1,2] Pisin Chen,[2,3,4,*] Guey-Lin Lin,[1,2] Robert Noble,[5] and Richard Sydora[6]

[1]Institute of Physics, National Chiao-Tung University, Hsinchu 300, Taiwan
[2]Leung Center for Cosmology and Particle Astrophysics, National Taiwan University, Taipei 106, Taiwan
[3]Department of Physics and Graduate Institute of Astrophysics, National Taiwan University, Taipei 106, Taiwan
[4]Kavli Institute for Particle Astrophysics and Cosmology, SLAC National Accelerator Laboratory, Menlo Park, California 94025, USA
[5]SLAC National Accelerator Laboratory, Menlo Park, California 94025, USA
[6]Department of Physics, University of Alberta, Edmonton, Alberta, Canada T6G 2G7
(Received 12 March 2008; published 17 March 2009)

Magnetowave induced plasma wakefield acceleration (MPWA) in a relativistic astrophysical outflow has been proposed as a viable mechanism for the acceleration of cosmic particles to ultrahigh energies. Here we present simulation results that clearly demonstrate the viability of this mechanism for the first time. We invoke the high frequency and high speed whistler mode for the driving pulse. The plasma wakefield obtained in the simulations compares favorably with our newly developed relativistic theory of the MPWA. We show that, under appropriate conditions, the plasma wakefield maintains very high coherence and can sustain high-gradient acceleration over hundreds of plasma skin depths. Invoking active galactic nuclei as the site, we show that MPWA production of ultrahigh energy cosmic rays beyond ZeV (10^{21} eV) is possible.

DOI: 10.1103/PhysRevLett.102.111101 PACS numbers: 98.70.Sa, 52.40.Db, 52.25.Xz, 52.65.Rr

The origin of ultrahigh energy cosmic rays (UHECR) has been a long-standing mystery in astrophysics. Thus far, the theories that attempt to explain the origin of UHECR can be broadly categorized into the ‘‘top-down’’ and the ‘‘bottom-up’’ scenarios. The top-down scenario resorts to the decay of some superheavy beyond the standard model particle, while the bottom-up scenario assumes the acceleration of an ordinary particle, such as a proton, at some astrophysical site to ultrahigh energies. Soon after the discovery of the cosmic microwave background (CMB), Greisen, Zatsepin, and Kuzmin (GZK) [1] showed that the high energy cosmic proton would lose its energy through interaction with the CMB, and as a result its spectrum would be subject to a cutoff. The decay of a superheavy particle locally, on the contrary, would not suffer the same fate. Precision measurements [2,3] on the yield of air-shower induced fluorescence lend support to the energy calibration of the HiRes observations [4]. Recent data from the Pierre Auger Observatory [5], also fluorescence normalized, exhibit a similar location of an ‘‘ankle’’ and the GZK suppression in HiRes. The observations of the GZK suppression weakens the argument for top-down exotic models. If these models are indeed disfavored, then the challenge to find a viable bottom-up mechanism to accelerate ordinary particles beyond 10^{20} eV becomes more acute.

Shocks, unipolar inductors, and magnetic flares are the three most potent, observed, ‘‘conventional’’ accelerators that can be extended to account for $\sim$ZeV($= 10^{21}$ eV) energy cosmic rays [6]. Radio jet termination shocks and gamma ray bursts have been invoked as sites for the shock acceleration, while dormant galactic center black holes and magnetars have been proposed as sites for the unipolar inductor acceleration and the flare acceleration, respectively. Each of these models, however, presents problems [6]. Evidently, novel acceleration mechanisms that can avoid some of the difficulties faced by these conventional models should not be overlooked.

Plasma wakefield accelerators [7,8] are known to possess two salient features: (i) The plasma can support an extremely high ‘‘acceleration gradient,’’ i.e., energy gain per unit distance, which does not depend (inversely) on the particle's instantaneous energy or momentum. This is essential to avoid the gradual decrease of efficiency in reaching ultrahigh energies. (ii) The acceleration field is collinear to the particle momentum. Therefore, bending of the trajectory is not a necessary ingredient in this mechanism. This helps to minimize inherent energy losses that would be severe at ultrahigh energies. Motivated by these considerations, it was proposed [9] that UHECR can be produced from the plasma wakefield excited by a ‘‘magnetowave’’ ($|B| > |E|$) in astrophysical outflows. Though attractive, this concept has never been validated through computer modeling. In this Letter, we present the relativistic magnetowave induced plasma wakefield acceleration (MPWA) theory and confirm such a concept by the plasma particle-in-cell (PIC) simulations.

Magnetized plasmas support a variety of wave modes propagating at arbitrary angles to the imposed magnetic field. For our purpose, we focus on wave modes propagating parallel to the external magnetic field to ensure the linear acceleration. In this case, the electromagnetic waves become circularly polarized, and the dispersion relation with the ionic motion neglected reads [10]

$$\omega^2 = k^2c^2 + \frac{\omega_p^2/\gamma}{1 \mp \omega_c/\omega\gamma}, \tag{1}$$

where the upper (lower) signs denote the right-hand (left-hand) circularly polarized waves, γ is the Lorentz factor of the electron quiver motion, $\omega_p = \sqrt{4\pi e^2 n_p/m_e}$ is the electron plasma frequency, and $\omega_c = eB/m_e c$ is the electron cyclotron frequency. The right-handed polarization has two real solutions with high and low frequency branches and has a frequency cutoff which forms a forbidden gap for wave propagation. The low frequency solution is called the whistler wave which propagates at a phase velocity less than the speed of light. When the magnetic field is sufficiently strong such that $\omega_c/\omega \gg \gamma$ and $\omega_c\omega/\omega_p^2 \gg 1$, the second term on the right-hand side of Eq. (1) is negligible. Hence the whistler mode has an approximately linear dispersion, and its phase velocity approaches to c. It is instructive to combine the two linearity conditions into a chain inequality: $(\omega_c'/\omega_p')^2 \gg \omega_c'/\omega \gg 1$, where $\omega_c' = \omega_c/\gamma$ and $\omega_p' = \omega_p/\sqrt{\gamma}$. Clearly, the range of ω compatible with this chain inequality increases with the ratio ω_c'/ω_p'. In other words, for a larger ω_c'/ω_p', the dispersion relation is approximately linear over a wider range of wave numbers (see Fig. 1). In this case, the traveling wave pulse can maintain its shape over a macroscopic distance, a condition favorable for the plasma wakefield acceleration.

Under the desirable condition where the phase velocity $v_{\rm ph} = \omega/k \sim v_g \sim c$, the plasma wakefield described by the normalized scalar potential $\phi(z,t) \equiv e\Phi(z,t)/m_e c^2$ can be solved from the following set of equations:

$$\frac{\partial^2\phi}{\partial z^2} = k_p^2\left(\frac{n}{n_0} - 1\right), \tag{2a}$$

$$\frac{\partial n}{\partial t} + c\frac{\partial}{\partial z}(n\beta_z) = 0, \tag{2b}$$

$$\frac{d}{dt}(\gamma\beta_\perp) = \frac{da}{dt} - i\omega_c\beta_\perp, \tag{2c}$$

$$\frac{d}{dt}(\gamma\beta_z) = c\frac{\partial\phi}{\partial z} - \frac{e}{mc^2}(v_xB_y - v_yB_x), \tag{2d}$$

$$\frac{d\gamma}{dt} = -\frac{e}{mc^2}(E_xv_x + E_yv_y + E_zv_z), \tag{2e}$$

where $a(z,t) \equiv eA(z,t)/m_ec^2 = eE_\perp/m_ec\omega$ is the normalized vector potential, customarily used to express the pulse intensity. For convenience, one can rewrite the above equations in terms of the comoving coordinates (ζ, τ), with $\zeta = z - v_gt$ and $\tau = t$. Hence, under the quasistatic approximation [11], the Maxwell equation $\nabla \times \boldsymbol{E} = -\partial\boldsymbol{B}/c\partial t$ leads to $E_x(\zeta) = B_y(\zeta)$ and $E_y(\zeta) = -B_x(\zeta)$. Applying Eq. (2e), Eq. (2d) can be simplified as

$$\frac{\partial}{\partial\zeta}[\phi - \gamma(1-\beta_z)] = 0, \tag{3}$$

which is in the same form as the unmagnetized plasma case. Integrating Eq. (2c) renders the following relation

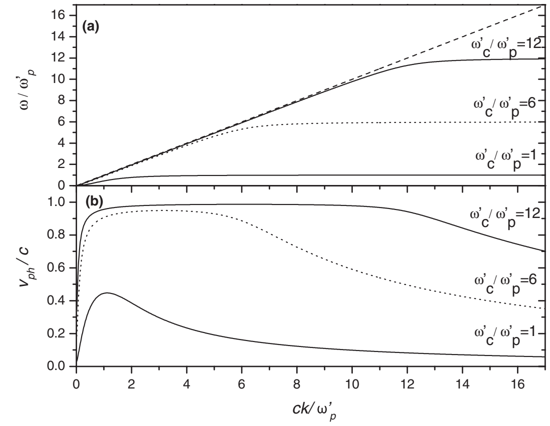

FIG. 1. (a) Frequency and (b) phase velocity versus wave number for different magnetic field strengths. Here $\omega_c' \equiv \omega_c/\gamma$ and $\omega_p' \equiv \omega_p/\sqrt{\gamma}$. When $\omega_c'/\omega_p' \gg 1$, the dispersion relation is approximately linear over a wider range of wave numbers with phase velocity approaching the speed of light.

among $\beta_\perp$, γ, and a:

$$\beta_\perp = \frac{a}{|\gamma - \frac{\omega_c}{\omega(1-\beta_z)}|}. \tag{4}$$

We note that the condition for a nonrelativistic plasma motion where $\beta_\perp \ll 1$ and $\beta_z \ll 1$ is $a \ll \omega_c/\omega - 1$.

By substituting Eq. (4) back into Eq. (3) and imposing the boundary conditions, the differential equation for the plasma wakefield becomes

$$\frac{\partial^2\phi}{\partial\zeta^2} = \frac{k_p^2}{2}\left[\left(\frac{a^2}{(1-\frac{\omega_c}{\omega(1+\phi)})^2} + 1\right)\frac{1}{(1+\phi)^2} - 1\right]. \tag{5}$$

The acceleration gradient $G = eE_z = -e\partial\phi/\partial\zeta$ can be calculated by solving the above differential equation. It is easy to see that Eq. (5) reduces to the previous results in the nonrelativistic limit $\phi \ll 1$ [12,13] and the unmagnetized limit $\omega_c \to 0$ [11]. In the nonrelativistic limit, the maximum acceleration gradient G in terms of the cold wave-breaking limit $E_{\rm wb} \equiv m_ec\omega_p/e$ and the strength parameter a_0 (the maximal value of a) is given by

$$G = \frac{a_0^2}{(1-\frac{\omega_c}{\omega})^2}\chi eE_{\rm wb}, \tag{6}$$

where χ is the form factor depending on the shape of the pulse.

We note that the right-hand side of Eq. (5) becomes singular as $1 + \phi \to \omega_c/\omega$. In such a limit, both the slope of E_z and the plasma density become infinite, which indicates the occurrence of wave breaking. Beyond this point, the plasma wave development is expected to become turbulent, and our fluid equation analysis will break down. The electric field is expected to remain finite since the amplitude of a relativistic plasma wave is proportional to $\sqrt{\gamma} = (1-\beta_{z,\max}^2)^{-1/4}$, where $\beta_{z,\max}$ is the maximum electron velocity in the wave. The above infinite-density situation would not occur if the strength parameter a_0 is smaller than an upper bound determined by the ratio ω_c/ω and the shape of the whistler pulse [14].

In order to confirm the analytical model of the acceleration gradient and investigate the dynamical behavior, we have conducted computer simulations of the MPWA process driven by a Gaussian whistler pulse. Our simulation model integrates the relativistic Newton-Lorentz equations of motion in the self-consistent electric and magnetic fields determined by the solution to Maxwell's equations [15,16]. The four-dimensional phase space (z, p_x, p_y, p_z) is used for the charged particle dynamics, and a uniform external magnetic field B_0 is imposed in the z direction. We used a wave packet with Gaussian width $\sigma = 80\Delta/\sqrt{2}$, where Δ is the cell size taken to be unity and the wave number $k = 2\pi/40\Delta$. The normalized physical parameters $\omega_c/\omega_p = 12$ and $m_i/m_e = 2000$ were taken, and for a uniform background plasma with electron collisionless skin depth $c/\omega_p\Delta = 30$, this gives $\omega/\omega_p = 4.64$ and $v_g/c \simeq \omega/ck = 0.986$. Other numerical parameters used are the total number of cells in the z direction $L_z = 2^{14}\Delta = 546c/\omega_p$, the average number of particles per cell was 10, and the time step $\omega_p\Delta t = 0.05$. The fields were normalized by $(1/30)E_{\text{wb}}$.

We set the maximum amplitude $E_{\perp 0} = 20$, which gives the strength parameter $a_0 = eE_{\perp 0}/m_e c\omega = 0.143 \ll \omega_c/\omega - 1$. Thus the wakefield in our simulation is in the linear regime with $\gamma \sim 1$. The pulse was initialized at $z_0 = 500\Delta = 16.66c/\omega_p$. To avoid spurious effects, we gradually ramped up the driving pulse amplitude until $t = 200\omega_p^{-1}$, during which the plasma feedback to the driving pulse was ignored. After these times, the driving pulse-plasma interaction was tracked self-consistently. As the dispersion relation is not perfectly linear, there should be a gradual spread of the pulse width. Thus $E_{\perp 0}$ of the driving pulse decreases accordingly. As a result, the maximum wakefield amplitude E_z declined in time. However, we have seen that such a degradation becomes milder as the ratio ω_c/ω_p increases [13]. The current study takes $\omega_c/\omega_p = 12$, which is sufficiently large that the wakefield maximum remains nearly constant even at $\Delta t = 300\omega_p^{-1}$ after the pulse was released (Fig. 2).

In Fig. 3, we show the $\omega - k$ intensity generated from the PIC simulation driving the pulse power spectrum. It is superimposed with the theoretical curve of the whistler wave dispersion relation for $\omega_c/\omega_p = 1$, 6, and 12. We confirm that the driving pulse is indeed the desirable whistler wave. Next, we validate the functional dependence of the acceleration gradient given by the solution of Eq. (5). Wave packets are initialized with a fixed wave number $k = 2\pi/60\Delta$. The pulse electric field $E_{\perp 0}$ is varied from 10 to 80. The strength parameter a_0 then varies accordingly. Figure 4 plots the acceleration gradient G versus a_0. The dashed curve is the extrapolation of the nonrelativistic result, Eq. (6), which is valid only in the $a_0 \ll \omega_c/\omega - 1$ limit. The simulation data points agree well

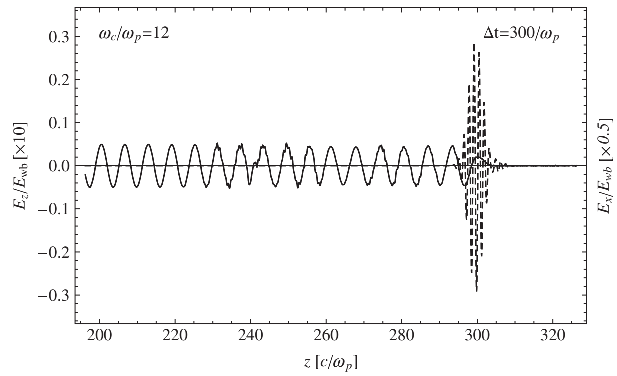

FIG. 2. A late time snapshot of the wakefield at $\Delta t = 300\omega_p^{-1}$.

instead with the solid curve obtained by solving Eq. (5) exactly.

We now apply the mechanism to the production of UHECR. First we note that a single encounter of the test particle with one wakefield can hardly accomplish the job of ushering the test particle to ultrahigh energy. Various degradation effects such as the dispersion of the driving magnetowave pulse and the phase slippage between the test particle and the wakefield would eventually throw the test particle out of the acceleration phase into the deceleration phase, and vice versa. Furthermore, the progenitor of the source is likely to burst out magnetoshocks or waves at random, which further aggravates the situation [17]. Therefore, in our vision the plasma wakefield-based cosmic accelerator would consist of numerous random acceleration and deceleration segments along certain astrophysical relativistic outflow, while each such acceleration segment is described by our MPWA model above.

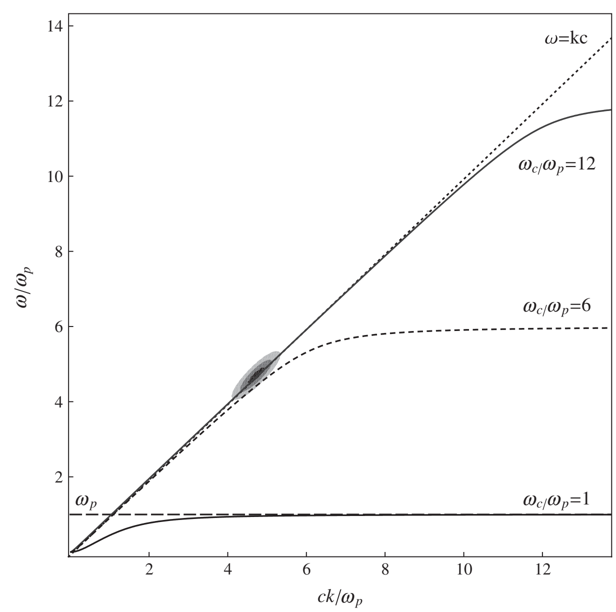

FIG. 3. The intensity contours of the driving pulse as a function of (ω, k) from PIC simulation. The light cone and the theoretical dispersion curves for the whistler wave with $\omega_c/\omega_p = 1$, 6, and 12 are superimposed.

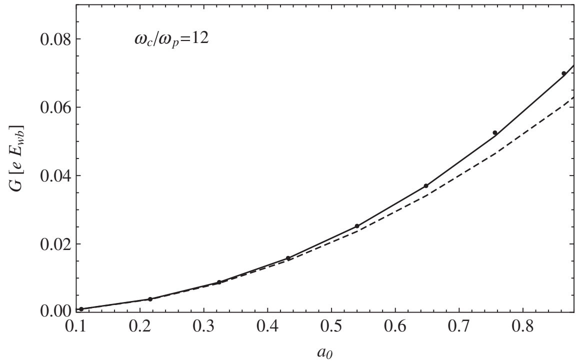

FIG. 4. The plot of accelerating gradient G versus a_0. The simulation data points agree well with the solid curve obtained by solving Eq. (5). The dashed curve is the extrapolation of the nonrelativistic theoretical result, Eq. (6).

As shown in Refs. [9,17], such stochastic encounters of the test particle with the random acceleration-deceleration phases would result in an inverse-square-law spectrum $f(\mathcal{E}) \propto 1/\mathcal{E}^2$. The various inevitable energy loss mechanisms would possibly degrade the power-law spectrum to $1/\mathcal{E}^{2+\beta}$, with $\beta > 0$. Phenomenologically, the allowed range for β can be determined by performing fittings to the measured UHECR spectrum [18].

Next we invoke active galactic nuclei (AGN) [19] as the site for the MPWA production of UHECR to illustrate the effectiveness of our mechanism. AGN typically release their energy through relativistic jets that extend a distance far greater than the size of the core with a negligible diverging angle. Typically, the total jet length can be a few kiloparsecs to megaparsecs. It is therefore appropriate to model the jet as a cylinder. As a consequence, the plasma density and the magnetic field strength remain constant over a large distance inside the jet. For an AGN with the central black hole mass $\sim 10^8 M_\odot$, it is reasonable to assume the plasma density $\sim 10^{10}$ cm^{-3} and the magnetic field $\sim 10^4$ G in the core [20], which gives $\omega_c/\omega_p \sim O(10^2)$ and the cold wave-breaking limit $E_{\rm wb} \sim 10^5$ V/cm. If we further assume that the AGN luminosity approaches the Eddington limit ($\sim 10^{46}$ erg/s) and that the AGN jet radius is comparable to the Schwarzschild radius of the central black hole, we then have $a_0 = \sqrt{4\pi\eta(E_{\rm AGN}^2/4\pi)(e/m_e c\omega)^2} \sim \sqrt{10\eta}$, where ω is taken to be $\sim\omega_c/2$ and η is the fraction of total energy imparted into the magnetowave modes. Since the frequency of the magnetowave in this case lies in the regime of radio waves, we assume that the observed AGN radio wave luminosity [21] is the result of the total mode conversion from the magnetoshocks at the same frequency. The ratio of radio wave luminosity to the total luminosity then gives $\eta \sim (10^{-3}\text{–}10^{-4})$ and $G \sim \mathcal{O}(10^2)$ eV/cm. Therefore, under the most optimized condition, particles would reach $E \sim 10^{21}$ eV in a distance ~ 3 pc, which is a tiny fraction of the typical AGN jet length.

We have newly developed the relativistic theory of MPWA and confirmed such a concept through PIC simulation. As a first step, we simulate the process with a Gaussian magnetowave profile. It is desirable to investigate our mechanism with magnetoshocks instead, which maybe astrophysically more relevant, and also investigate the generation of magnetoshocks in the plasma outflows. Aside from its application to a cosmic accelerator, MPWA may also be of interest as a fundamental phenomenon in plasma physics and as an alternative approach to terrestrial plasma wakefield accelerators [13].

This work is supported by the U.S. DOE (Contract No. DE-AC03-76SF00515), the National Science Council of Taiwan (Grants No. 95-2119-M-009-026 and No. 97-2112-M-002-026-MY3), and the Natural Sciences and Engineering Research Council of Canada.

*chen@slac.stanford.edu

[1] K. Greisen, Phys. Rev. Lett. **16**, 748 (1966); G. T. Zatsepin and V. A. Kuzmin, JETP Lett. **4**, 78 (1966).

[2] J. Belz *et al.* (FLASH Collaboration), Astropart. Phys. **25**, 57 (2006).

[3] M. Ave *et al.* (AIRFLY Collaboration), arXiv:astro-ph/0703132.

[4] R. U. Abbasi *et al.* (HiRes Collaboration), Phys. Rev. Lett. **100**, 101101 (2008).

[5] J. Abraham *et al.* (Pierre Auger Collaboration), Phys. Rev. Lett. **101**, 061101 (2008).

[6] R. Blandford, Phys. Scr. **T85**, 191 (2000); arXiv:astro-ph/9906026.

[7] T. Tajima and J. M. Dawson, Phys. Rev. Lett. **43**, 267 (1979).

[8] P. Chen *et al.*, Phys. Rev. Lett. **54**, 693 (1985).

[9] P. Chen, T. Tajima, and Y. Takahashi, Phys. Rev. Lett. **89**, 161101 (2002).

[10] L. Stenflo, Phys. Scr. **14**, 320 (1976).

[11] P. Sprangle, E. Esarey, and A. Ting, Phys. Rev. A **41**, 4463 (1990).

[12] P. K. Shukla, Phys. Scr. **T52**, 73 (1994).

[13] P. Chen, F. Y. Chang, G. L. Lin, R. J. Noble, and R. Sydora, Plasma Phys. Controlled Fusion **51**, 024012 (2009); arXiv:0808.3036.

[14] F. Y. Chang *et al.* (to be published).

[15] J. M. Dawson, Rev. Mod. Phys. **55**, 403 (1983).

[16] R. D. Sydora, J. Comput. Appl. Math. **109**, 243 (1999).

[17] P. Chen, T. Tajima, and Y. Takahashi, arXiv:astro-ph/0205287.

[18] See, for example, D. De Marco and T. Stanev, Phys. Rev. D **72**, 081301 (2005).

[19] There have been recent discussions on the correlation of UHECR with AGN by the Pierre Auger Collaboration: J. Abraham *et al.*, Science **318**, 939 (2007); Astropart. Phys. **29**, 188 (2008); **30**, 45 (2008); and the HiRes group: R. U. Abbasi *et al.*, *ibid.* **30**, 175 (2008).

[20] M. J. Rees, M. C. Begelman, and R. D. Blandford, Ann. N.Y. Acad. Sci. **375**, 254 (1981).

[21] T. Arshakian, E. Ros, and A. Zensus, arXiv:astro-ph/0608172.